

Supporting Information (SI)

Effective Synthesis of $\text{Pb}_5\text{S}_2\text{I}_6$ Crystals at Low Temperature for Fabrication of a High Performance Photodetector

Hongrui Wang,^{†,‡,§,∥} Guihuan Chen,^{†,‡,§,∥} Jianhang Xu,[#] Yunpeng Xu[‡] and Qing Yang^{*,†,‡,§,∥}

[†]Hefei National Laboratory of Physical Sciences at the Microscale, [‡]Department of Chemistry, [§]Laboratory of Nanomaterials for Energy Conversion, and [∥]Synergetic Innovation Center of Quantum Information & Quantum Physics, University of Science and Technology of China, Hefei 230026, Anhui, P. R. China

[#] Department of Physics, College of Science and Technology, Temple University, Philadelphia 19122-1801, Pennsylvania, the USA.

E-mail: qyoung@ustc.edu.cn; Fax: +86-551-63606266; Tel: +86-551-63600243.

Characterization Methods. The structure and purity of the $\text{Pb}_5\text{S}_2\text{I}_6$ crystals was characterized by powder X-ray diffraction (XRD), which was carried out on a Philips X'Pert Pro Super diffractometer using a source of graphite monochromatized $\text{Cu K}\alpha$ radiation ($\lambda = 1.54178 \text{ \AA}$).^{S1} The size and morphology of the samples was observed by field-emission scanning electron microscopy (FESEM), which was performed on a JEOL JSM-6700F.^{S2} Meanwhile, X-ray photoelectron spectroscopy (XPS) was carried out to determine the chemical status of the as-obtained $\text{Pb}_5\text{S}_2\text{I}_6$ crystals by using a VGESCA LAB MKII X-ray photoelectron spectrometer,^{S3} of which monochromatic $\text{Al K}\alpha$ X-ray is served as the excitation source. In addition, Raman spectrum of the $\text{Pb}_5\text{S}_2\text{I}_6$ crystals was recorded by using a JYLABRAM HR Confocal Laser Micro Raman spectrometer using source of 514.5 nm generated by an argon laser, and UV-Vis-NIR absorption spectrum of the crystals was collected using a Perkin Elmer Lambda 950 UV-Vis-NIR spectrophotometer.^{S4}

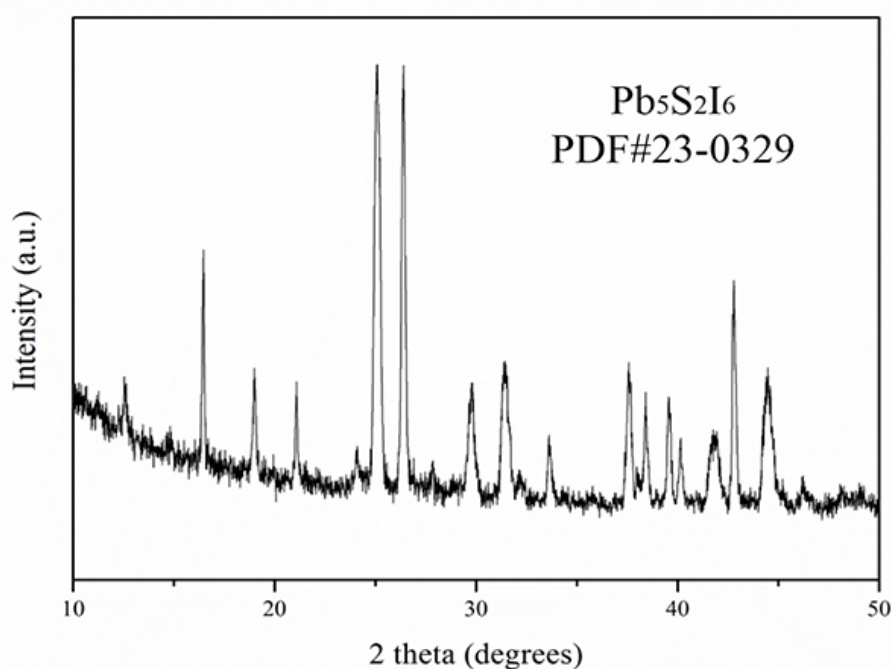


Figure S1. XRD pattern of the sample synthesized at 160 °C for 10 h in 0.8 mol L^{-1} hydrochloric acid.

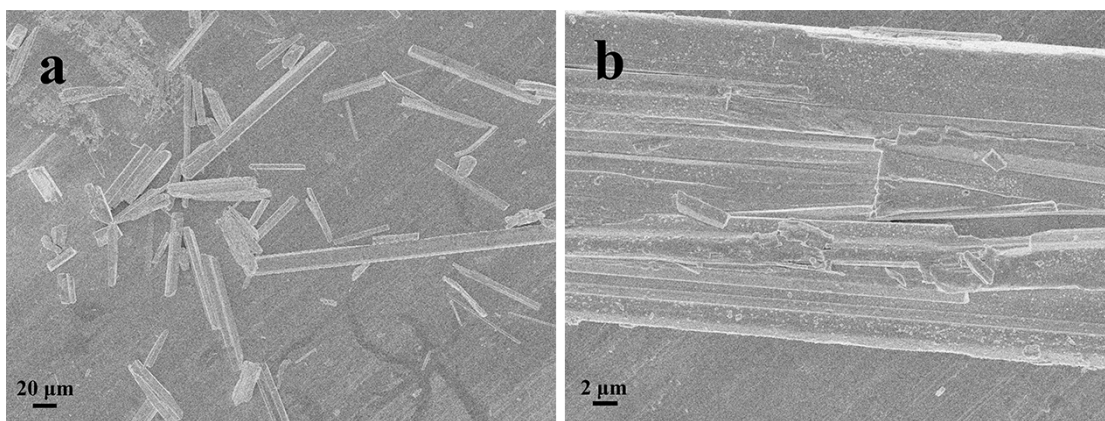


Figure S2. (a) Low- and (b) high-magnification SEM images of the $\text{Pb}_5\text{S}_2\text{I}_6$ crystals synthesized at $160\text{ }^\circ\text{C}$.

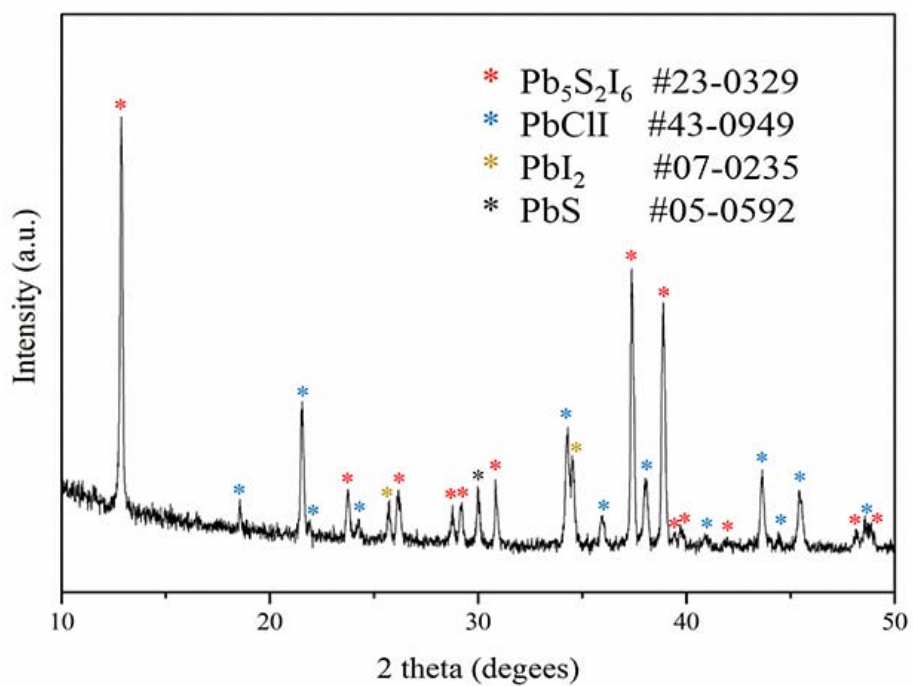


Figure S3. XRD pattern of the sample synthesized at $160\text{ }^\circ\text{C}$ for 4 h in 0.8 mol L^{-1} hydrochloric acid.

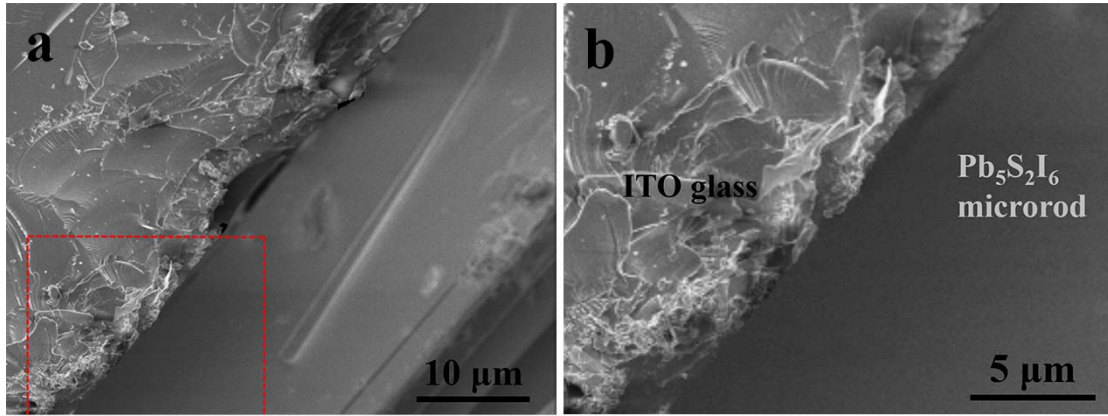


Figure S4. (a) Typical SEM image for the optoelectronic device, taken at contact area of electrode between the individual $\text{Pb}_5\text{S}_2\text{I}_6$ single crystal and the ITO substrate glass, and (b) the corresponding magnified image for the selected region in (a).

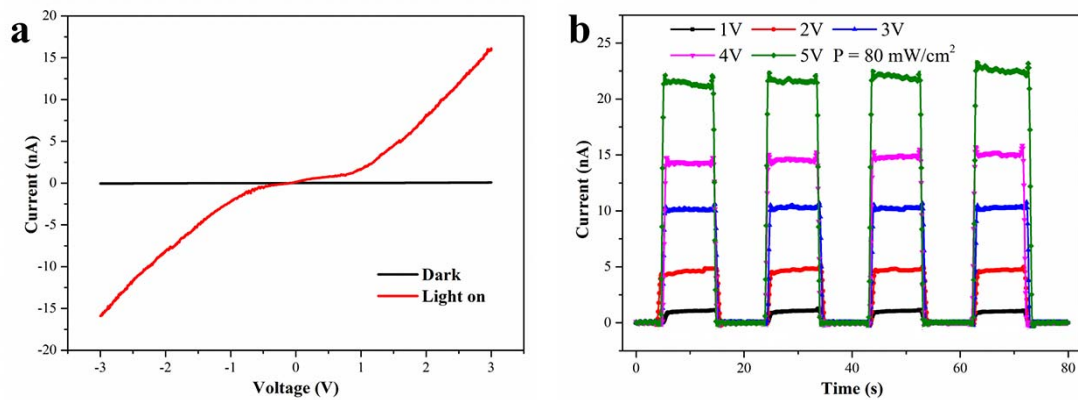


Figure S5. (a) The I-V curves of the device (made by silver electrodes) in dark and light, and (b) the time function of the on-off photocurrent response of the device at different bias voltage.

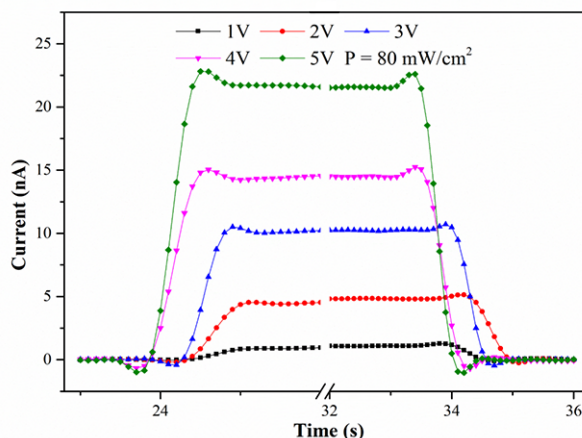


Figure S6. The response/recovery time of the photodevice constructed by silver electrodes (under 80 mW cm^{-2} illumination).

For comparison, we have measured the photodetective performances of the photodevice constructed by silver electrodes, as demonstrated in Figure S5. In typical, the wavelength of incident light was 200-2500 nm, generated from Xe lamp without using any filter to simulate the sunlight, during all measurements at room temperature (300 K). As seen in Figure S5a, the I-V characteristics suggest that there are Schottky contacts between the $\text{Pb}_5\text{S}_2\text{I}_6$ microrod and silver paints, and the results are consistent with the ones performed on ITO glass in the manuscript (Figure 7). Figure S5b displays the photoresponse switch behavior of the new photodetector tested by periodically turn on and off the light (80 mW cm^{-2}) at the bias voltage from 1 V to 5 V, and it is found that there is a rapid response and good stability for the photodetector. However, when we magnifies Figure S5b to Figure S6, it is easy to be found that the response and recovery time of the new photodetector are about less than 0.7 s, which is larger than the typical result performed on ITO glass in the manuscript (0.2 s, Figure 7 and Table 1).

Supplementary Reference

S1 Wang, W.; Zhang, L.; Chen, G.; Jiang, J.; Ding, T.; Zuo, J.; Yang, Q. Cu_{2-x}Se Nanooctahedra: Controllable Synthesis and Optoelectronic Properties. *CrystEngComm* **2015**, *17*, 1975-1981.

S2 Jing, Z.; Zhan, J. Fabrication and Gas-Sensing Properties of Porous ZnO Nanoplates. *Adv. Mater.* **2008**, *20*, 4547-4551.

S3 Xiong, S.; Xi, B.; Wang, C.; Xi, G.; Liu, X.; Qian, Y. Solution-Phase Synthesis and High Photocatalytic Activity of Wurtzite ZnSe Ultrathin Nanobelts: A General Route to 1D Semiconductor Nanostructured Materials. *Chem.-Eur. J.* **2007**, *13*, 7926-7932.

S4 Li, Y.; Guo, Y.; Tan, R.; Cui, P.; Li, Y.; Song, W. Synthesis of SnO₂ Nanosheets by a Template-Free Hydrothermal Method. *Mater. Lett.* **2008**, *63*, 2085-2088.